Ultrafast OH production in clusters containing N_2O and HI

P. I. Ionov,[a] S. I. Ionov,[b] and C. Wittig
Department of Chemistry, University of Southern California, Los Angeles, California 90089-0482

(Received 28 July 1997; accepted 19 August 1997)

The geometrical arrangement of reagents is an important factor influencing chemical reactions in condensed phases and molecular clusters. In the present study, OH buildup times have been recorded upon photolysis of $(N_2O)_m(HI)_n$ clusters in order to elucidate the role of the cluster environment on the reaction mechanism. The buildup times were measured for different molecular beam compositions (i.e., degrees of clustering). The buildup time changed from $\leqslant 100$ fs at the lowest backing pressures (119 and 132 kPa) to 430 fs at 188 kPa. It is argued that at the lower backing pressures the OH derives primarily from binary N_2O-HI complexes. However, regardless of the cluster species involved, the fast OH buildup at the lowest backing pressures suggests a dominant direct oxygen abstraction mechanism rather than reaction via a vibrationally excited intermediate such as $HNNO^{\dagger}$. © *1997 American Institute of Physics.* [S0021-9606(97)00744-7]

I. INTRODUCTION

An important feature of photoinitiated reactions in weakly bound clusters is the initial spatial arrangement provided by these environments. Unlike reactions that take place in the homogeneous gas phase, where all impact parameters and mutual orientations of the reactants are equally possible, the orientations of the clustered moieties and the impact parameters of the photoprepared reactants are dictated by the geometrical properties of the parent cluster. This suggests the possibility of changing reaction pathways in cluster environments—an idea which is responsible for much of the present interest in photoinitiated processes in weakly bound clusters.[1]

An intriguing example is the case of N_2O-HI binary clusters. Here, photoinitiated reactions of H atoms with N_2O have as options chemically distinct product channels such as NH+NO+I and N_2+OH+I as well as different mechanistic pathways leading to the same chemical products. A simple way of envisioning this is to consider direct abstraction versus the formation and subsequent decomposition of an $HNNO^{\dagger}$ vibrationally excited intermediate:

$$N_2O\text{-}HI + h\nu \rightarrow N_2 + OH + I \quad \text{(direct)} \tag{1}$$

$$\rightarrow HNNO^{\dagger} + I, \tag{2}$$

followed by

$$HNNO^{\dagger} + I \rightarrow N_2 + OH + I \tag{3}$$

$$\rightarrow NH + NO + I, \tag{4}$$

where reaction (3) occurs via a 1,3-hydrogen shift mechanism.

Given the complexity of cluster environments, it should be understood from the outset that reactions (1)–(4) denote a highly simplified scheme whose purpose is to provide qualitative guidance. Other sets of products such as NHI+NO, NH+INO, and N_2+HOI are energetically accessible and cannot be ruled out a priori. Moreover, species such as NHI, INO, and HOI may participate as short-lived intermediates which decompose. However, they require more active participation of the I atom than do reactions (1)–(4), and therefore we assume that they are of secondary importance, as discussed below. The product channels depicted in reactions (1)–(4) are inferred from the corresponding gas phase reactions, which have been studied both experimentally and theoretically[2,3]:

$$H + N_2O \rightarrow N_2 + OH(\text{direct}) \tag{5}$$

$$\rightarrow HNNO^{\dagger}, \tag{6}$$

followed by

$$HNNO^{\dagger} \rightarrow N_2 + OH \tag{7}$$

$$\rightarrow NH + NO. \tag{8}$$

The primary means of studying these gas phase reactions experimentally has involved the use of fast hydrogen atoms. Alternatively, the reaction of NH with NO has been examined by Dagdigian and co-workers,[4] who showed that the reaction transpires via the HNNO intermediate.

Based on an intuitive correspondence between the gas phase and cluster reactions, the latter can be thought of as occurring in two steps. Namely, HI is optically excited to its repulsive electronic state, yielding fast hydrogen, which then reacts with the nearby N_2O. From this perspective, reactions (5)–(8) are the second and essential part of the cluster reactions. Despite its intuitive appeal, this picture is crude, primarily because it neglects the role of the nearby iodine. Though the close proximity of the iodine atom may complicate the chemistry, we will try to glean as much information as possible from the correspondence between the cluster and gas phase reactions.

As seen from the potential energy versus reaction coordinate diagram shown in Fig. 1,[2] in the case of the gas phase reaction there are two distinct paths leading to OH. One is

[a]Present address: Applied Materials, 3320 Scott Blvd., M.S. 1114, Santa Clara, CA 95054.
[b]Present address: Hughes Research Labs, 3011 Malibu Canyon Road, M.S. RL65, Malibu, CA 90265.

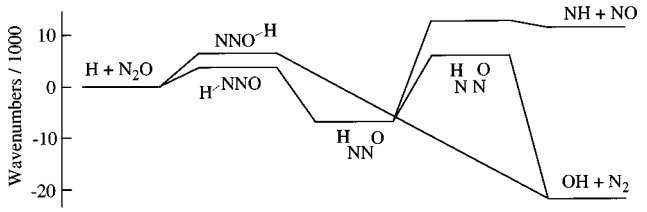

FIG. 1. Stationary points of the HNNO potential energy surface (see Ref. 2).

direct oxygen abstraction, which takes the order of a vibrational period to occur, while the other proceeds through the $HNNO^{\dagger}$ intermediate and therefore takes longer. Thus, if biases due to the cluster geometry cause the system to prefer one or the other of these possibilities, recording the time-resolved OH buildup may enable us to distinguish between the two mechanisms. This is the focus of the present study.

Under gas phase conditions, OH production is thought to involve the $HNNO^{\dagger}$ intermediate as per reaction (7), though the contribution of this channel relative to reaction (5) has not been established definitively. Marshall *et al.*[3] measured and calculated thermal rates, $k(T)$, for reactions (5)–(7). They were able to fit their experimental rates with the calculated ones over a broad temperature range and found the $HNNO^{\dagger}$ intermediate to be the major pathway for temperatures $\leqslant 2000$ K. Böhmer *et al.*[5] subsequently recorded product state distributions for the reaction of 300 K N_2O with fast hydrogen atoms produced by HI photolysis. They found significant N_2 vibrational excitation and attributed this to the participation of the $HNNO^{\dagger}$ intermediate, in which case OH is formed by a 1,3-hydrogen shift mechanism. These authors invoked a simple Franck–Condon model in which the N_2 vibrational distribution is estimated by projecting a transition state wave function onto the N_2 vibrations. Thus, the different N–N bond lengths in N_2 versus the 1,3-hydrogen shift transition state (i.e., 1.10 vs 1.23 Å) were deemed responsible for the large amount of product N_2 vibrational excitation. This straightforward estimate was able to reconcile the experimental result. However, since the sudden approximation invoked is extreme, the agreement obtained is not conclusive insofar as mechanism is concerned.

The large amount of N_2 vibrational excitation reported by Böhmer *et al.* could not be reproduced by the study of Bradley *et al.*,[6] who calculated trajectories and found considerably less N_2 vibrational excitation for reactions that proceed via the $HNNO^{\dagger}$ intermediate. This discrepancy remains unexplained. On the one hand, despite some flexibility of the theoretical result, the theoretically determined PES could not be adjusted to make the theoretical and experimental results agree.[7] Moreover, these authors have had good success with other four-atom systems, and such a large difference with experiment is without precedent in their previous studies. On the other hand, the most obvious experimental shortcoming (i.e., collisions of the OH) would have increased the estimate of the N_2 vibrational excitation, making the difference between experiment and theory even larger.

In the cluster environment, it is likely that the mechanism is biased toward the direct reaction. Böhmer *et al.* observed an order of magnitude decrease in the [NH]/[OH] ratio when reaction was photoinitiated in clusters versus the gas phase (at the same wavelength).[5] It was considered unlikely that so large a change in the product channel branching ratio could be explained by just the squeezed atom effect acting in the binary cluster.[1] The squeezed atom effect increases the product center-of-mass translational energy at the expense of product internal energies in cluster versus gas phase reactions, and therefore it discriminates against the higher energy NH+NO channel. However, an order-of-magnitude change in the [NH]/[OH] ratio is not anticipated. Since NH is produced only through the $HNNO^{\dagger}$ intermediate, the smaller relative NH yield is in accord with the mechanism having switched to a predominantly direct process. One has to be cautious, however, in attributing the Böhmer *et al.* results to binary clusters, as higher-than-binary clusters may have been abundant under their experimental conditions.

If the cluster reaction indeed forms OH via the direct path, it is intuitive that hydrogen initially lies closer to the oxygen than to the terminal nitrogen. Though the N_2O-HI geometry has not been established experimentally, other N_2O-HX clusters (X=F,Cl,Br) have been studied both theoretically and experimentally, the latter by using high-resolution IR spectroscopy.[8] The progression of cluster geometries for different halogens allows one to make an educated guess of the N_2O-HI geometry. Two isomers, one linear with hydrogen attached to the terminal nitrogen (XH-NNO) and one bent with hydrogen attached to the oxygen (NNO-HX), are predicted theoretically for F and Cl. However, the linear isomer has been observed experimentally only for N_2O-HF,[9] and its stability has been shown to be far less than for the other isomer, NNO-HF. With the other N_2O-HX clusters (X=Cl and Br), only the bent NNO-HX forms have been observed experimentally. Note also, the bent isomers become progressively more inertially *T*-shaped (i.e., the halogen facing the central nitrogen) as the halogen becomes heavier. Extrapolating this trend to HI suggests that in N_2O-HI the iodine faces the central nitrogen. Also, calculations predict that the hydrogen favors the oxygen in N_2O-HX clusters,[8,10] which makes it tempting to assume that this is also the case in N_2O-HI. Note that HI differs considerably from other HX molecules, having a small dipole moment and large polarizability, and we expect the H atom to be highly delocalized in the N_2O-HI cluster. Nonetheless, even a very large zero-point amplitude can still accommodate a preference for the oxygen side over the terminal nitrogen side. Such a geometry should favor the direct oxygen abstraction mechanism, which would be consistent with the dramatic decrease in the NH production in the experiment of Böhmer *et al.*

Thus, the modest number of experimental and theoretical studies carried out to date suggest that cluster-induced specificity is a possibility. This is examined in the present experiment by measuring the OH buildup times in photoinitiated cluster reactions.

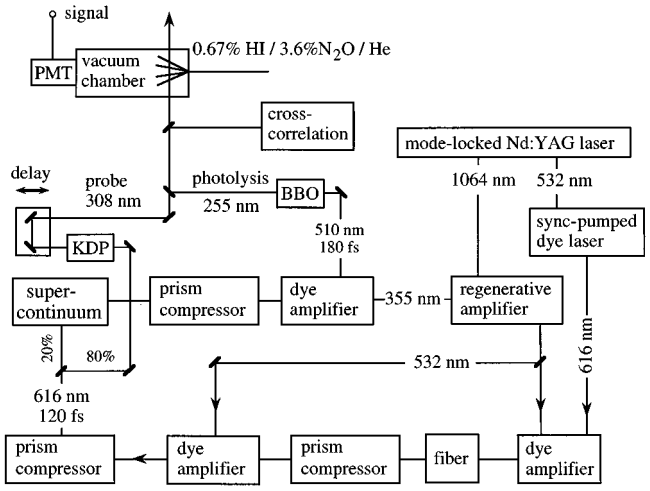

FIG. 2. Block diagram of the experimental arrangement.

II. EXPERIMENT

Continuous progress in ultrafast laser technology creates new possibilities in different areas of chemistry and physics every year.[11] Whereas pulse durations of 10–30 fs have been achieved throughout the visible,[12,13] two-color pump-probe experiments,[14] and especially experiments in the ultraviolet,[15,16] pose additional challenges. These difficulties are exacerbated by the high average laser powers needed to study processes such as bimolecular reactions in clusters, which involve small concentrations and low probability events. These complications result in longer pump-probe cross correlations than would be achieved at longer wavelengths and with high density samples.

The present experiment is a compromise between shortening the pump-probe cross correlations and maintaining sufficient laser energies to obtain measurable signals (i.e., typically 0.2–0.5 counts per laser pulse). Due to photon statistics, smaller signals result in lower S/N, thereby reducing the accuracy of the measured buildup times. Only by shortening the cross-correlation widths simultaneously with increasing the pump and probe energies was it possible to improve the accuracy of the buildup times.

Despite numerous modifications to the laser system since our previous experiment,[17] the method has remained the same conceptually. Reaction is initiated by fast H atoms produced by the 255 nm photolysis of clusters containing HI and N_2O, and the OH product is detected by using 308 nm laser-induced fluorescence (LIF). The LIF signal is recorded versus pump-probe delay. To achieve the best time resolution for a given pulse duration, we simultaneously recorded the cross correlation. This was used in the fitting procedure to account for the finite pulse durations and the pump-probe delay jitter. Accuracy of the method was tested with a benchmark system: direct H_2O_2 photodissociation.[18]

The laser arrangement is shown in Fig. 2. It provides $\sim 15\ \mu$J of 255 nm pump and 20–50 μJ of 308 nm probe radiation with cross-correlation widths of ~ 300 fs at the lower range of outputs and ~ 400 fs at maximum output. Seed pulses are selected from a synchronously pumped dual jet dye laser (Coherent 700) and are amplified in a 10 Hz red dye amplifier. Spectrally-selected supercontinuum serves as the input for the blue-green amplifier. The dye laser operates on Kiton Red and DQTCI saturable absorber in ethylene glycol and is pumped by the doubled output of a mode-locked Nd:YAG laser (Spectron SL903). Saturation was minimized in both dye amplifiers by maximizing beam cross sections in the dye cells. For the same reason, three instead of two amplification stages were used in the blue-green amplifier.[17] Coumarin 503 in methanol was used for the blue amplifier and Sulfphorhodamine 640 in a 1:1 mixture of water and methanol was used for the red amplifier. A 1 mm RG 695 Schott filter served as a saturable absorber after the first stage of the red amplifier. To reduce saturation and improve the beam profile, a noncollinear geometry[19] was implemented in the first stage of the blue-green amplifier. Both amplifiers were pumped by a Continuum RGA-69-10 regenerative amplifier.

Fiber stretching and compression were used to shorten the seed pulse.[20] First, the seed (~ 1 nJ, 0.8 ps autocorrelation width) is preamplified by a factor of 20–100 in a dye cell with variable amplification before coupling it into a single-mode polarization preserving fiber (3.3 μm core diam., 86 mm length). Thus, effects of long-term seed intensity variation are compensated by constantly monitoring the fiber throughput and adjusting the amplification of the preamplifier. The coupling efficiency of a freshly cleaved fiber is $\sim 60\%$.

The pulse that has been chirped in the fiber is compressed in a double pass prism compressor.[21] Two more prism compressors are used to compensate for group velocity dispersion in the amplifiers and other optics, one after the red amplifier and the other before the blue-green amplifier. All three compressors consist of 60° SF10 prisms; since 60° is the Brewster angle, reflection losses are minimal. Note also that two compressors are needed (before and after the red amplifier) because of the saturable absorber. The negative group velocity dispersion is partitioned between the two compressors such that minimum pulse duration is achieved in the saturable absorber. This yields the shortest amplified pulse.

The 510 nm seed for the blue amplifier is selected from a supercontinuum[22] generated in 3 mm quartz. As pointed out by others,[23] we find that in order to preserve coherence of the supercontinuum it has to be generated near threshold and the seed has to be spatially homogeneous. Thus, only 20% of the amplified 616 nm light is taken and a homogeneous portion of this beam is selected with 2 mm diaphragm. This radiation is focused into the quartz with a 30 cm lens. 510 nm radiation is selected from the white light by a single cavity interference filter with a 230 cm^{-1} bandwidth. Typical autocorrelations that correspond to 0.5 and 0.3 mJ of the red and blue-green amplifiers outputs respectively are shown in Fig. 3. We believe that broadening of the blue pulse as compared to the red one is primarily due to high-order phase distortions in the filter, since autocorrelations measured without frequency selection are narrower than those of the red

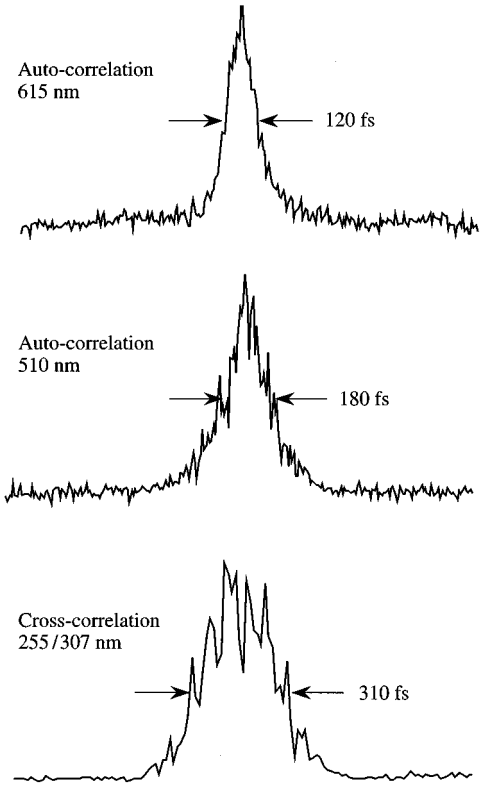

FIG. 3. Typical auto and cross correlations under similar experimental conditions.

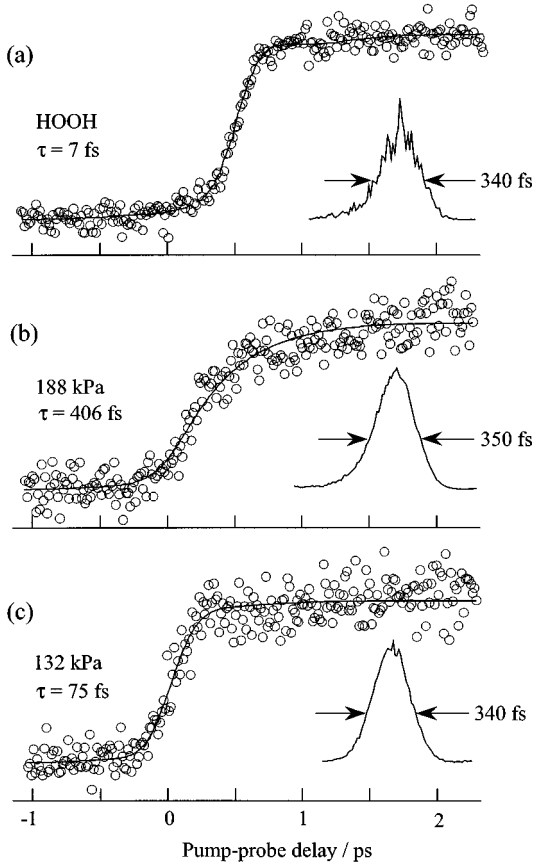

FIG. 4. OH LIF and cross correlation signals versus delay; circles represent data and solid lines are the best fits; (a) hydrogen peroxide; (b) $(N_2O)_m(HI)_n$ at 188 kPa backing pressure; (c) $(N_2O)_m(HI)_n$ at 132 kPa backing pressure.

seed. Even longer cross correlations (also shown in Fig. 3) are tentatively attributed to the delay jitter of the white light relative to its seed.

Group velocity mismatch of the fundamental and the harmonic in a doubling crystal leads to increased duration of the harmonic.[24] To minimize this, thin crystals were used for doubling, autocorrelation, and cross-correlation measurements. To obtain better conversion efficiencies the fundamentals were focused just below the self focusing threshold. 250 μm KDP doubles the red beam and 100 μm BBO doubles the blue beam, while 90 μm BBO is used to measure the cross correlation. The cross correlation is recorded simultaneously with the LIF signal by directing the Fresnel reflection from the vacuum chamber window ($\sim$15%) into a BBO crystal. The difference frequency is detected by a Ge photodiode. To compensate for different group velocity dispersion in the LIF and the cross-correlation arms, a quartz plate is placed in the cross-correlation arm. Fresnel reflection off the plate are used to measure pump and probe energies by Si photodiodes.

Clusters are produced in a free jet expansion. A mixture of 0.67% HI, 3.5% N_2O, and 95.83% He is expanded through a 1 mm$\times$0.1 mm pulsed nozzle at backing pressures of 119–188 kPa. A small portion around the jet axis is directed into a quadrupole mass spectrometer. The cluster ions N_2OHI^+, $N_2O(HI)_2^+$, and $(N_2O)_2HI^+$ are observed, and the ratios $[N_2O(HI)_2^+]/[N_2OHI^+]$ and $[(N_2O)_2HI^+]/[N_2OHI^+]$ change from 0.17 to 0.22 as the stagnation pressure is increased from 130 to 160 kPa.

The 255 nm pump and 308 nm probe are focused onto the molecular beam and LIF is collected by an $f/1$ quartz lens. A 308 nm interference filter in front of the PMT blocks background radiation. Though it attenuates the pump-probe signal by a factor of 4, it is essential because some of the background signals are time dependent.[17] Typical LIF signals are 0.2–0.5 photon counts per laser pulse.

Since the pump-probe cross correlation is used in the fitting of the data, the overall time resolution is better than the cross-correlation width and is determined by the accuracy of the cross-correlation and the degree to which the fitting function describes the data. As in our previous experiment,[17] time resolution was checked by measuring direct H_2O_2 photodissociation, which is essentially instantaneous at our time resolution. H_2O_2 is introduced into the chamber in a continuous flow through a separate inlet. Since it does not pass through the pulsed nozzle, there is no H_2O_2 contamination. The OH LIF signal in the case of H_2O_2 is recorded under the same conditions as for the case of $(N_2O)_n(HI)_m$. It was found that OH buildup from H_2O_2 was best fitted with time constants <50 fs.

III. RESULTS

Figure 4 shows typical OH LIF signals versus pump-

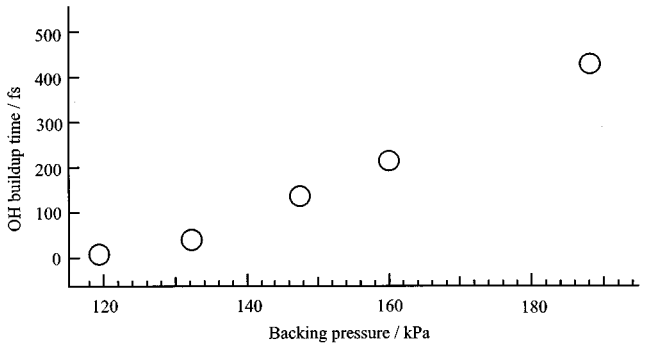

FIG. 5. OH buildup time vs nozzle backing pressure for photolysis of $(N_2O)_m(HI)_n$ clusters.

probe delay for H_2O_2 photodissociation and for photoinitiated reactions in $(N_2O)_m(HI)_n$ clusters. The signals rise monotonically with delay and do not exhibit coherent effects. The pump-probe cross correlation is measured simultaneously with the OH LIF signals and is approximately 350 fs FWHM.

The quality of the data does not justify the extraction of more than a single fitting parameter characterizing the buildup. It is assumed that OH buildup is exponential, which cannot be justified theoretically, at least for direct dissociation. Nevertheless, this ad hoc assumption provides a measure of an upper bound for the lifetime of the reaction intermediate. Also, in order to account for the laser pulse durations, the single exponential buildup was convoluted with the experimentally measured cross-correlation by using the functional form:

$$S(t) \propto \int_{-\infty}^{t} dt' R(t') \left[1 - \exp\left(- \frac{t-t'}{\tau} \right) \right], \tag{9}$$

where $R(t)$ is the experimentally determined cross correlation. The fits thus obtained are presented in Fig. 4 as solid lines. The quality of the fits suggests that the assumptions, as well as the functional form $S(t)$, are as good as the experimental data.

To examine the dependence of the OH buildup time on the composition of the nozzle effluent (i.e., degree of clustering), the backing pressure was lowered from 188 to 119 kPa, at which point the signal almost disappeared. The dependence of the buildup time on backing pressure is shown in Fig. 5. Measurement uncertainties are such that the smallest OH buildup times (at pressures of 119 and 132 kPa) are certainly less than 125 fs and probably less than 100 fs; in round numbers, we give this as $\leqslant$100 fs. The OH buildup time increases with backing pressure, which suggests a qualitative dependence on average cluster size: the larger the cluster, the longer the OH buildup time.

IV. DISCUSSION

A significant finding is the increase of the OH buildup time from $\leqslant$100 to 400 fs upon increasing the nozzle backing pressure from 119 to 188 kPa. This behavior differs qualitatively from that of the CO_2/HI system, where it was found that the OH buildup times did not change over a wide range of backing pressures.[17] The essential contribution of this paper is the presentation of the data and a discussion of possible reaction pathways. Relevant issues include: (i) which cluster species are responsible for the signals; (ii) what are the effects of cluster geometry; (iii) is selectivity achieved; and (iv) is it meaningful to compare the gas phase and cluster reactions, and if so, what conclusions can be drawn from these comparisons.

The first step toward determining the mechanisms responsible for OH production in the present work is establishing the identity of the cluster species involved in producing OH. Due to the unselective nature of the experiment, all of the cluster species present in the expansion and containing at least one molecule each of N_2O and HI can, in principle, participate in OH production. However, a number of factors suggest that, at the lowest backing pressures, the OH signals derive primarily from binary clusters.

One suggestion comes from mass spectra of the nozzle effluent. Only dimer and trimer clusters ions were observed. Tetramer cluster ions were not observed despite good sensitivity. Also, the concentrations of the trimer cluster ions were lower than those of the dimer cluster ions, the ratio being 0.17–0.22 for the pressure range 130–160 kPa. It is tempting to attribute the lower concentrations of the larger cluster ions to lower concentrations of the larger neutral clusters. However, because the cracking patterns of the neutral clusters are unknown, the mass spectra are only suggestive of a primary role for neutral dimers.

Another piece of evidence which suggests that small clusters are responsible for the low-backing-pressure signals is the short OH buildup time of $\leqslant$100 fs. This suggests a direct process, which is more likely to occur in small clusters where the number of attack parameters is less numerous than in large clusters. Also, energy dissipation and caging in larger clusters would tend to lengthen OH buildup times.[25] These considerations suggest that product buildup times increase with average cluster size (and therefore with backing pressure) in accord with our data. This does not prove that binary clusters are the source of the low-backing-pressure signals, though this hypothesis seems reasonable. However, if binary clusters are not responsible for the OH detected in our experiments, the discussion that follows is applicable, for the most part, to those clusters which are responsible for the low-pressure signals. This would be the case, for example, if N_2O-HI produces relatively little OH compared to a trimer such as $(N_2O)_2HI$.

Even if OH derives from binary clusters at the lowest backing pressures, interpreting the $\leqslant$100 fs buildup time is not straightforward, since the available structural and dynamical information is only indirectly relevant to the N_2O-HI system. As mentioned above, structure is inferred from other N_2O-HX clusters and dynamical information is available only for the gas phase $H+N_2O$ reaction. Thus, the knowledge base for this system is sparse.

Photoexcited N_2O-HI is truly a five-atom system and if rigorous dynamics are to be considered it should be viewed

as such. Unfortunately, a nine-dimensional PES is required (ignoring vibration-rotation coupling), whose construction is daunting. Therefore, we will attempt to first exploit the analogy with the gas phase $H+N_2O$ reaction. As mentioned above, one extreme is to consider iodine as a spectator that does not strongly influence the dynamics. An argument in favor of this is that the experiment is only sensitive to OH, whose production is determined by intracluster ''collisions'' of hydrogen with N_2O. Since the equilibrium separation of the clustered moieties is large compared to chemical bond lengths, photoexcitation can expand the HI bond before the hydrogen ''encounters'' nearby N_2O. In this sense, photodissociation and reaction are seen as serial events. The fact that the hydrogen is initially going away from the iodine argues against subsequent interactions between the iodine atom and the other four atoms.

On the other hand, the rapid OH buildup of $\leqslant 100$ fs precludes the possibility of a strong case being made for the iodine spectator model. The spectator approximation is most applicable when the non-participating atom leaves the interaction region quickly relative to the time scale of the reaction. This holds for CO_2-HI, where the OH buildup rates have been shown to be $\leqslant 4\times 10^{12}$ s^{-1}.[17] However, it is not true for the present N_2O-HI experiments. The separation between the I atom and the other moiety that can be achieved within 100 fs can be estimated by assuming that some fraction of the available energy goes into relative translation. For instance, with a reduced mass of 33 amu and 1000 cm^{-1} in relative translation (corresponding to less than 7% of the available energy), the separation increases by only 0.9 Å in 100 fs. Thus, for modest translational energies, the I atom stays in the vicinity of the other four atoms during OH buildup.

Such close proximity of I leads to additional interactions during the reaction. For example, there is an attractive N-I interaction between I and HNNO and the possibility of forming species such as HNI, INO, and HOI (either above or below their dissociation energies) cannot be excluded. However, it is important to note that the participation of such intermediates is expected to lengthen, not shorten, OH buildup times.

On time scales of 100 fs or shorter, there can be no simple relationship between the rates of reactions that produce OH and the experimentally determined OH buildup times. Specifically, the OH cannot be formed, escape its surroundings, and be detected by LIF in so short a time. For example, an OH moiety traveling at 10^5 cm s^{-1} moves only 1 Å in 100 fs. Since its $A\ ^2\Sigma^+$ excited state can be quenched by the immediate $I+N_2$ environment, this places a lower bound on the LIF measurement of OH buildup times which has nothing to do with the chemistry that produces OH. At short times such as $\leqslant 100$ fs, the system is molecular soup.

As discussed in the Introduction, it is possible that the dominant mechanism of the cluster reaction could be established by comparing the experimental OH buildup time with the calculated lifetime of the $HNNO^\dagger$ intermediate. This was the original goal of the present study. The buildup time of $\leqslant 100$ fs is shorter than the 600 fs $HNNO^\dagger$ lifetime calculated by Bradley *et al.*[6] who used the method of classical trajectories. This suggests that the cluster reaction does not go through the $HNNO^\dagger$ intermediate but proceeds via direct attack at the oxygen. However, to say with more certainty that the $HNNO^\dagger$ intermediate is not involved in the reaction, a lower bound for its lifetime is needed. Simonson *et al.*[26] performed RRKM calculations and obtained lifetimes less than 200 fs when anharmonicity was not included. By varying the anharmonicity it was possible to increase the lifetime to 600 fs but it is not clear whether such large anharmonicity is realistic. Another important issue that was not addressed in the calculations is the participation of excited electronic surfaces. In earlier work, OH $A\ ^2\Sigma^+ \rightarrow X\ ^2\Pi$ emission was observed following collisions of H atoms with N_2O.[5] This was a clear indication that excited PESs are involved, though the extent and mechanisms of their participation were not established.

The above considerations lead us to conclude that the lower bound to the $HNNO^\dagger$ lifetime is still an open issue. Thus, it is premature to accept unequivocally reaction (1) as the dominant mechanism, though, of the various choices, it is the one most consistent with the available information.

To summarize, OH buildup is observed on a $\leqslant 100$ fs time scale following the 255 nm photolysis of a free jet expansion containing clusters of HI an N_2O. At the lowest backing pressures, it is likely that the OH arises from photoinitiated reaction in binary N_2O-HI clusters. If the calculated 600 fs lifetime of the $HNNO^\dagger$ intermediate is verified, then the $\leqslant 100$ fs OH buildup time observed in the present experiments suggests that the cluster reaction proceeds via direct oxygen abstraction.

ACKNOWLEDGMENTS

This research was supported by the National Science Foundation. Discussions with G. C. Schatz have influenced the thinking on this problem.

[1] Y. Chen, G. Hoffmann, S. K. Shin, D. Oh, S. Sharpe, Y. P. Zeng, R. A. Beaudet, and C. Wittig, in *Advances in Molecular Vibrations and Collisions* (JAI, 1991), Vol. 1B, pp. 187–229, and references therein.
[2] S. P. Walch, J. Chem. Phys. **98**, 1170 (1993).
[3] P. Marshall, A. Fontijn, and C. F. Melius, J. Chem. Phys. **86**, 5540 (1987).
[4] D. Patel-Misra and P. Dagdigian, J. Phys. Chem. **96**, 3232 (1992).
[5] E. Böhmer, S. K. Shin, Y. Chen, and C. Wittig, J. Chem. Phys. **97**, 2536 (1992).
[6] K. S. Bradley, P. McCabe, G. C. Schatz, and S. P. Walch, J. Chem. Phys. **102**, 6696 (1995).
[7] G. C. Schatz (private communications).
[8] Y. P. Zeng, S. W. Sharpe, D. Reifschneider, C. Wittig, and R. A. Beaudet, J. Chem. Phys. **93**, 183 (1990).
[9] C. M. Lovejoy and D. J. Nesbitt, J. Chem. Phys. **90**, 4671 (1989).
[10] S. K. Shin, C. Wittig, and W. A. Goddard III (unpublished).
[11] *Special Issue on Ultrafast Optics and Electronics*, IEEE J. Quantum Electron. **QE-28**, 2084 (1993).
[12] R. W. Schoenlein, J.-Y. Bigot, M. T. Portella, and C. V. Shank, Appl. Phys. Lett. **58**, 801 (1990).
[13] P. Simon, S. Szatmari, and F. P. Schäfer, Opt. Lett. **20**, 1569 (1991).
[14] W. Sibbett, R. S. Grant, and D. E. Spence, Appl. Phys. B **58**, 171 (1994).
[15] G. Rodriguez, J. P. Roberts, and A. J. Taylor, Opt. Lett. **19**, 1146 (1994).
[16] J. Ringling, O. Kittelmann, F. Noack, G. Korn, and J. Squier, Opt. Lett. **18**, 2035 (1993).

[17] S. I. Ionov, G. A. Brucker, C. Jaques, L. Valachovic, and C. Wittig, J. Chem. Phys. **99**, 6553 (1993).
[18] H. Okabe, *Photochemistry of Small Molecules* (Wiley, New York, 1978).
[19] S. Szatmari, G. Almasi, and P. Simon, Appl. Phys. B **53**, 82 (1991).
[20] W. J. Tomlinson, R. H. Stolen, and C. V. Shank, J. Opt. Soc. Am. B **1**, 139 (1984).
[21] R. L. Fork, O. E. Martinez, and J. P. Gordon, Opt. Lett. **9**, 150 (1984).
[22] R. L. Fork, C. V. Shank, C. Hirlimann, R. Yen, and W. J. Tomlinson, Opt. Lett. **8**, 1 (1983).
[23] J. H. Glownia, D. R. Gnass, and P. P. Sorokin, J. Opt. Soc. Am. B **11**, 2427 (1994).
[24] I. V. Tomov, R. Fedosejevs, and A. A. Offenberger, IEEE J. Quantum Electron. **QE-18**, 2048 (1982).
[25] R. Alimi and R. B. Gerber, Phys. Rev. Lett. **64**, 1453 (1990).
[26] M. Simonson, K. S. Bradley, and G. C. Schatz, Chem. Phys. Lett. **244**, 19 (1995).